Available online at www.sciencedirect.com
ScienceDirect
Continental Shelf Research 26 (2006) 2125–2140
CONTINENTAL SHELF RESEARCH
www.elsevier.com/locate/csr

# Nature of decadal-scale sediment accumulation on the western shelf of the Mississippi River delta

D. Reide Corbett[a,*], Brent McKee[b,1], Mead Allison[b]

[a]*Department of Geological Sciences, Coastal Resources Management, East Carolina University, Greenville, NC 27858, 252-328-1367, USA*
[b]*Department of Earth and Environmental Sciences, Tulane University, New Orleans, LA 70118, 504-862-3167, USA*

Available online 1 September 2006

**Abstract**

Sediment delivered to coastal systems by rivers ($15 \times 10^9$ tons) plays a key role in the global carbon and nutrient cycles, as deltas and continental shelves are considered to be the main repositories of organic matter in marine sediments. The Mississippi River, delivering more than 60% of the total dissolved and suspended materials from the conterminous US, dominates coastal and margin processes in the northern Gulf of Mexico. Draining approximately 41% of the conterminous US, the Mississippi and Atchafalaya river system deliver approximately $2 \times 10^8$ tons of suspended matter to the northern Gulf shelf each year. Unlike previous work, this study provides a comprehensive evaluation of sediment accumulation covering majority of the shelf (<150 m water depth) west of the Mississippi Delta from 92 cores collected throughout the last 15 years. This provides a unique and invaluable data set of the spatial and modern temporal variations of the sediment accumulation in this dynamic coastal environment.

Three types of $^{210}$Pb profiles were observed from short cores (15–45 cm) collected on the shelf. Proximal to Southwest Pass in 30–100 m water depths, non-steady-state profiles were observed indicating rapid accumulation. Sediment accumulation rates in this area are typically $>2.5\,\mathrm{cm\,yr^{-1}}$ ($>1.8\,\mathrm{g\,cm^{-2}\,yr^{-1}}$). Kasten cores (~200 cm in length) collected near Southwest Pass also indicate rapid deposition ($>4\,\mathrm{cm\,yr^{-1}}$; $>3\,\mathrm{g\,cm^{-2}\,yr^{-1}}$) on a longer timescale than that captured in the box cores. Near shore (<20 m), profiles are dominated by sediments reworked by waves and currents with no accumulation (the exception is an area just south of Barataria Bay where accumulation occurs). The remainder of the shelf (distal of Southwest Pass) is dominated by steady-state accumulation beneath a ~10-cm thick mixed layer. Sediment accumulation rates for the distal shelf are typically $<0.7\,\mathrm{cm\,yr^{-1}}$ ($<0.5\,\mathrm{g\,cm^{-2}\,yr^{-1}}$). A preliminary sediment budget based on the distribution of $^{210}$Pb accumulation rates indicates that 40–50% of the sediment delivered by the river is transported out of the study region. Sediment is moved to distal regions of the shelf/slope through two different mechanisms. Along-isobath sediment movement occurs by normal resuspension processes west of the delta, whereas delivery of sediments south and southwest of the delta may be also be influenced by mass movement events on varying timescales.


*Keywords:* Radioisotope; Lead; Cesium; Sedimentation; Resuspension; Mississippi river; Sediment transport

## 1. Introduction

Continental margins play a significant role in the exchange of material between the continents and the open ocean. Many researchers have recognized

*Corresponding author. Tel.: +1 252 328 1367; fax: +1 252 328 4391.
*E-mail addresses:* corbettd@ecu.edu (D. Reide Corbett), bmckee@unc.edu (B. McKee), malliso@tulane.edu (M. Allison).
[1]Curent address: The University of North Carolina at Chapel Hill, Department of Marine Sciences, CB 3300, 12-7 Venable Hall, Chapel Hill, NC 27599-3300, USA.

0278-4343/$ - see front matter 
doi:10.1016/j.csr.2006.07.012

the disproportionately important role that river-dominated ocean margin systems may have in the delivery of dissolved and particulate materials to the coastal ocean (Dagg et al., 2004; McKee et al., 2004 and references therein). Rivers deliver approximately $15 \times 10^9$ tons of sediment to coastal margins each year. The world's 25 largest rivers account for approximately 40% of the fluvial sediments entering the ocean (Milliman and Meade, 1983; Meade, 1996). Sediment delivery to coastal systems plays a key role in the global carbon and nutrient cycles as deltas and continental shelves are considered to be the main repositories of organic matter in the ocean (Berner, 1982, 1989; McKee et al., 2004). The amount of particulate material delivered to the river's delta may differ significantly from the actual amount of material retained within the subaerial and subaqueous delta. These differences may be important in the cycling of biogeochemically active elements (i.e., C, N, etc.).

In many coastal systems, sediments are not simply permanently deposited on the shelf near the river mouth. As Wright and Nittrouer (1995) demonstrated, river-derived sediments may undergo several cycles of transport, deposition, and remobilization before reaching a long-term burial site. On energetic shelves with high particulate fluxes, sediments often form a surface ephemeral layer that is physically mixed, with only a fraction being buried on the longer term (Corbett et al., 2004; McKee et al., 2004). The concept of deposition versus permanent burial (accumulation) is a matter of timescale (McKee et al., 1983). The range in benthic residence time of organic material will impact the efficiency of remineralization and burial of carbon (McKee et al., 2004). The dynamic character of river-dominated ocean margin environments allows for significantly greater organic matter processing relative to other coastal systems (Aller, 1998). Therefore, it is important to understand the varying sedimentary processes and environments in these systems to further our knowledge of the fate of particulate material and geochemical constituents.

While extensive work has been conducted on the geologic framework of the Mississippi delta (Trowbridge, 1930; Fisk et al., 1954; Coleman and Gagliano, 1964; Penland and Boyd, 1981; Coleman, 1988; Coleman et al., 1998a and references therein), no systematic study of recent sediment accumulation patterns necessary to address aforementioned issues has been conducted, except in the Atchafalaya system (Neill and Allison, 2005). This paper presents results from several multidisciplinary studies of the shelf adjacent to the Mississippi River delta conducted in the late 1980s through the present. These studies included the Louisiana stimulus for excellence in research (LaSER; NSF-OCE and Louisiana board of reagents), Nutrient enhanced coastal ocean productivity (NECOP; NOAA), Mississippi River interdisciplinary research (MiRIR; DoD) project, and an NSF integrated carbon cycle (ICC; NSF) project. The goals of this paper are to quantify the rates of modern sediment accumulation on decadal timescales throughout the shelf adjacent to the Mississippi River delta, evaluate major processes that control the observed burial pattern, and to provide a sediment budget to account for the suspended-sediment load delivered by the lower Mississippi River.

## 2. Study area

The Mississippi is a major world river that dominates coastal processes in the northern Gulf of Mexico. It has the third largest drainage basin area and the seventh largest water discharge and suspended load among the world's rivers (Milliman and Meade, 1983; Meade, 1996). Approximately 60% of the total suspended matter and 66% of the total dissolved load transported from the conterminous US to the ocean is carried by the Mississippi–Atchafalaya River system (Presley et al., 1980). Draining approximately 41% of the conterminous US, the Mississippi and Atchafalaya rivers deliver approximately $210 \times 10^6$ metric tons (t) of suspended matter to the shelf of the northern Gulf of Mexico each year, of which $130–150 \times 10^6$ t is transported through the Mississippi's birdsfoot delta (measured at Tarbert Landing, 495 km upriver from the river mouth; Milliman and Meade, 1983; Meade and Parker, 1985; Meade, 1996; Mossa, 1996).

The Mississippi River has an average freshwater discharge of $380\,km^3\,yr^{-1}$ (measured at Tarbert Landing) through the distributaries of its birdfoot delta, directing freshwater input primarily to the west onto the Louisiana continental shelf (Meade and Parker, 1985). Streamflow in the lower Mississippi is influenced by a diversion of up to 30% (18–28%; Mossa, 1996) of total flow to the Atchafalaya River through a controlled diversion system just above Tarbert Landing. In nearly all years, mean Mississippi water discharge during the high-water months can be expected to be about three times the discharge during the low-water months (Meade, 1995). Sediments of the Mississippi are delivered through the birdfoot delta directly onto the continental shelf. Sediment delivered to the Mississippi delta has been significantly reduced due to the construction of dams, diversions, and levees; the suspended sediment load carried to the Gulf of Mexico has decreased by approximately one half since the 1800s, the majority of that occurring since 1950 (Keown et al., 1986; Mossa, 1996).

Sands delivered to the Mississippi delta are initially deposited within four channel widths seaward of the distributary mouths to produce the prograding distributary-mouth-bar (Wright and Coleman, 1974; Coleman, 1988). Fine-grained materials are delivered farther afield and more uniformly distributed to produce the prodelta muds (Coleman, 1981; Adams et al., 1987). Wright and Nittrouer (1995) suggested that the low oceanographic energy regime (i.e., low, near-bottom currents and along-shelf flows; Adams et al., 1982; Wiseman and Dinnel, 1988) of the continental shelf adjacent to the Mississippi River delta make it an end-member system. Consequently, there is little initial transport of river-borne material beyond ~30 km of the mouth of Southwest Pass. However, relatively large waves associated with winter frontal passages can remobilize sediments from the inner shelf of south Louisiana and transport them further west along the shelf following the dominant strong westward coastal current (Cochrane and Kelly, 1986; Cho et al., 1998) or off-shelf (Allison et al., 2000; Corbett et al., 2004). In addition, delta front failure, primarily driven by rapid sediment accumulation, differential loading of coarse sediments on the prodelta muds, excess pore pressure, and rapid biochemical degradation, is an active process that remobilizes a significant amount of material downslope (Prior and Coleman, 1978; Roberts et al., 1980; Adams and Roberts, 1993; Coleman et al., 1998b). This mass movement of sediment takes place in the form of slides, slumps, and growth faults on the prodelta, even with slopes as low as 0.2–0.5° (Coleman, 1988).

## 3. Materials and methods

### 3.1. Sampling

Box cores were collected on the shelf west of Southwest Pass during several cruises conducted aboard the R/V *Pelican* over the last decade. The majority of the box core data presented herein are from the LASER (April, 1989) and MiRIR (October–November 2000) cruises. Approximately 100 box cores were collected at 54 different stations on the shelf adjacent to the Mississippi River delta during these cruises. Samples were collected from seven across-shelf transects west of Southwest pass, as well as from stations within, south, and east of the birdfoot delta (Fig. 1). Longer cores (up to 3 m) from selected stations were collected in 2000 (MiRIR) and 2003 (ICC) using a kasten-type gravity corer to examine the sedimentary record on a longer timescale.

Box cores were subsampled with a 10-cm (diameter) plexiglass core tube and extruded at 0.5–2.0 cm intervals for radiochemical analysis and sedimentological properties. X-radiography was only conducted on the cores collected during the MiRIR cruises. Kasten cores were X-rayed by removing a 4 cm thick slab from the core, and the remainder was subsampled at 2-cm intervals downcore. Samples for porosity from box and kasten cores were collected and sealed in sample vials onboard at the time of initial sampling. A measured volume of wet sediment from each interval, typically 10 mL, was transferred to a preweighed container that was sealed and brought back to laboratory. These samples were oven dried at 60 °C for several days, and the gravimetrically determined water content, corrected for salt residue, was used to calculate the sediment dry-bulk density.

### 3.2. Radiometric analyses

$^{210}$Pb activities were determined by gamma and/or alpha counting. Samples analyzed by direct gamma counting were initially dried at 60 °C, homogenized by grinding, packed into standardized vessels, and sealed before counting for at least 24 h. Sample size ranged between approximately 2 and 40 g, depending on counting geometry (vial or tin, respectively). Gamma counting was conducted on one of the three low-background, high-efficiency, high-purity Germanium detectors (Coaxial-, BEGe-, and Well-type) coupled with a multi-channel analyzer. Detectors were calibrated using a natural matrix standard (IAEA-300) at each energy of interest in the standard counting geometry for the associated detector. Activities are corrected for self adsorption using a direct transmission method (Cutshall et al., 1983; Cable et al., 2001).

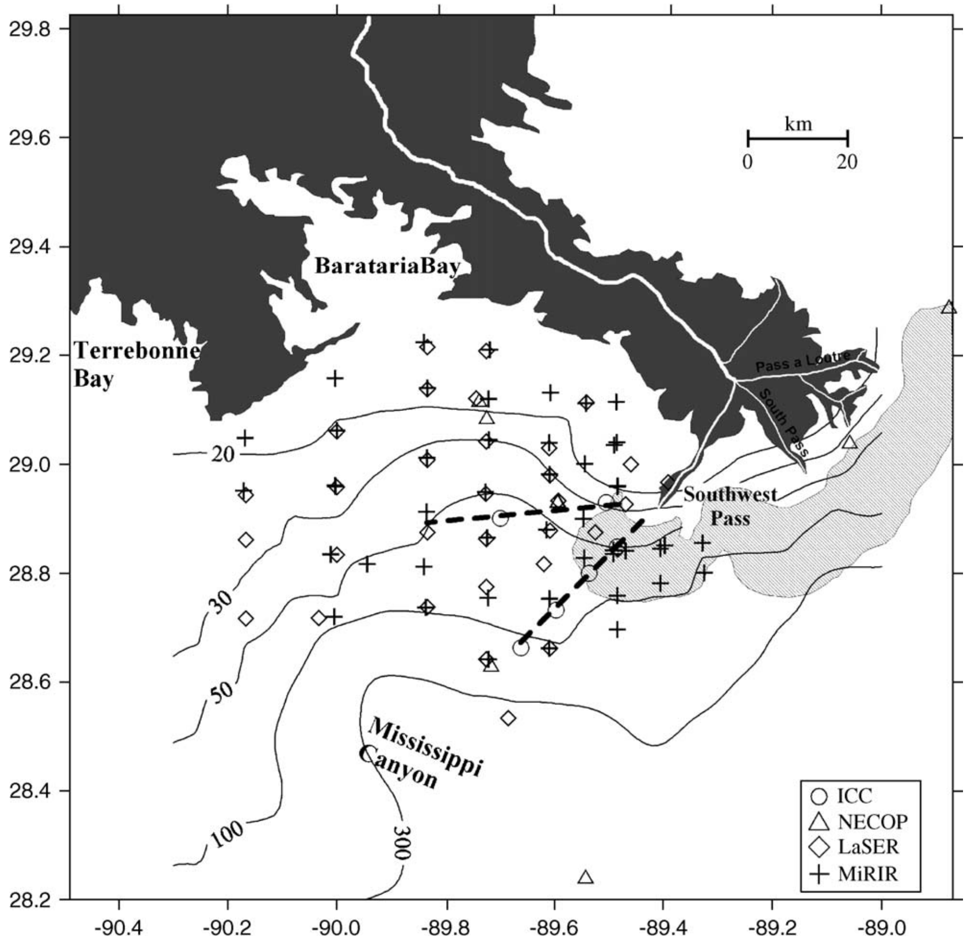


Fig. 1. Map of the study area showing box cores collected during the corresponding cruises: O—ICC (July 2003); Δ—NECOP (August 1990, February 1991, April 1992); ◇—LaSER (April 1988); + – MiRIR (April, October 2000). Several kasten cores were also collected proximal to the delta. Isobaths are in meters. The black dashed lines represent ship-track of seismic data collection. Hatched area represents approximate zone of mass sediment movement from Coleman (1988).

For those samples analyzed by gamma, $^{137}$Cs and $^{226}$Ra were also quantified. $^{137}$Cs activities were measured using the net counts at the 661.7 keV photopeak. $^{226}$Ra activities were determined via gamma spectrometry by allowing samples to equilibrate for greater than three weeks and recounting. $^{226}$Ra is then determined indirectly by counting the gamma emissions of its grand daughters, $^{214}$Pb (295 and 351 keV) and $^{214}$Bi (609 keV).

Total $^{210}$Pb measured by alpha spectroscopy followed the methodology of Nittrouer et al. (1979). Approximately 1.5 g of sediment was spiked with $^{209}$Po, a yield determinant, and partially digested with 8N $HNO_3$ by microwave heating. $^{210,209}$Po from the solution was then electrodeposited onto nickel planchets in a dilute acid solution (modified from Flynn, 1968). When using the alpha method, excess $^{210}$Pb activities were determined by subtracting the $^{210}$Pb activity supported by $^{226}$Ra from the total $^{210}$Pb activity. Supported $^{210}$Pb activities were assumed to be equal to the uniform background values found at depth in total $^{210}$Pb profiles or equal to the total $^{210}$Pb activity of the deepest sample when a constant background was not reached. These values were also cross-checked with adjacent cores where obvious background levels were observed.

### 3.3. *Seismic profiling*

Seismic transects were collected on cruises of the R/V *Eugenie* in April 2003 and the R/V *Pelican* in July 2003 (Fig. 1; dashed lines). Transects were made with an Edgetech X-star 1-12 kHz CHIRP subbottom profiler, a mid-depth towed system capable of 6–10 cm vertical resolution to a sub-bottom depth of 20–100 m depending on lithology. Seismic lines were recorded digitally and filtered in the laboratory to reduce noise and optimize gains. Transect location was determined by differential GPS corrected for fish layback from the receiver.

### 3.4. Calculation of sediment accumulation rates

The main processes governing excess $^{210}$Pb profiles are sediment accumulation, radioactive decay, and particle mixing (Goldberg and Koide, 1962). Therefore, processes other than radioactive decay can result in an exponential decrease of $^{210}$Pb, primarily a function of physical and biological mixing. Dividing the $^{210}$Pb profile into two layers, a surface mixed layer extending to some depth in the sediment profile above a zone of no mixing, allows the sediment accumulation rate to be calculated in the region of limited mixing via

$$A_x = A_0 e^{-\lambda x/S}, \quad (1)$$

where $A_x$ and $A_0$ (dpm L$^{-1}$) represents the excess $^{210}$Pb activity at depth $x$ (cm) and the sediment water interface (or at the boundary of the mixed layer), respectively; $S$ is the linear sediment accumulation rate (cm yr$^{-1}$); and $\lambda$ is the decay constant of $^{210}$Pb (0.031 yr$^{-1}$) (Appleby and Oldfield, 1992). Calculating the sediment accumulation rate below the mixing zone assumes that particle reworking rates are not significant over the depth interval of calculation, and that fluxes of both sediment and $^{210}$Pb have been constant over the age of the core. If deep mixing cannot be ruled out, Eq. (1) provides an upper limit of sediment accumulation (Benninger et al., 1979; Nittrouer et al., 1984). A mass accumulation rate (g m$^{-2}$ yr$^{-1}$) can also be calculated with Eq. (1) by plotting activities as a function of accumulated mass (g cm$^{-2}$) rather than linear depth (cm).

For several cores collected on the shelf, the above model (eg. Eq. (1)) is not applicable since there is essentially no change in excess $^{210}$Pb activity with depth (i.e., rapid deposition). Following Jaeger et al. (1998), we instead calculated minimum accumulation rates by dividing the deepest cored intervals (containing excess activity) by the maximum age for which excess $^{210}$Pb can be detected (~100 years). However, because these calculations are based on relatively short box cores (<40 cm core length), the actual accumulation rates are likely to be significantly higher.

Downcore $^{137}$Cs activities were generally used to substantiate the $^{210}$Pb-determined accumulation rates. Wherever possible the first appearance (1952; $^{137}$Cs horizon) or peak (1963) of $^{137}$Cs activity was used to estimate a sediment accumulation rate. In many cases the $^{137}$Cs activity was detectable throughout the core and therefore only a minimum accumulation rate could be estimated.

Finally, sediment accumulation rates were estimated from the subbottom depths of seismic reflectors observed in the two CHIRP seismic profiles. The reflectors were located within the upper 3 m of the seafloor. The sediment accumulation rates along each of the CHIRP profiles was determined assuming the age of reflector calculated from $^{210}$Pb data collected at one or more coring sites along the same transect and the thickness of sediment overlying the reflector at the same location. Assuming that the age of the reflector is constant along the profile, which is valid if these reflectors represent individual Mississippi River flood horizons, then along-profile accumulation rates (i.e., thickness/time) are interpolated between core locations and extrapolated elsewhere not obscured by gas.

## 4. Results and discussion

### 4.1. Depositional environments

Excess $^{210}$Pb profiles from box cores collected on the shelf were easily delineated into three types that provide insight to different depositional environments along the shelf. Following Aller (2001) and McKee et al. (2004), these profiles can be described by: (I) a zone of rapid accumulation; (II) no accumulation with an erosional surface reworked by waves and currents and a surface bioturbated zone (typically <10 cm); and (III) a surface mixed layer of homogenous excess $^{210}$Pb activity underlain by a steadily accumulating deposit. X-radiography and textural data (logged during core extrusion) provided additional insight into this classification (Fig. 2). Cores designated as having a zone of rapid accumulation (Type I) typically had X-radiographs with very little internal structure (e.g., massive) and no indication of macrofaunal burrows (Fig. 2a). Porosities of Type I environments showed little downcore change. In contrast, sites with no accumulation (Type II) exhibit a dramatic decrease

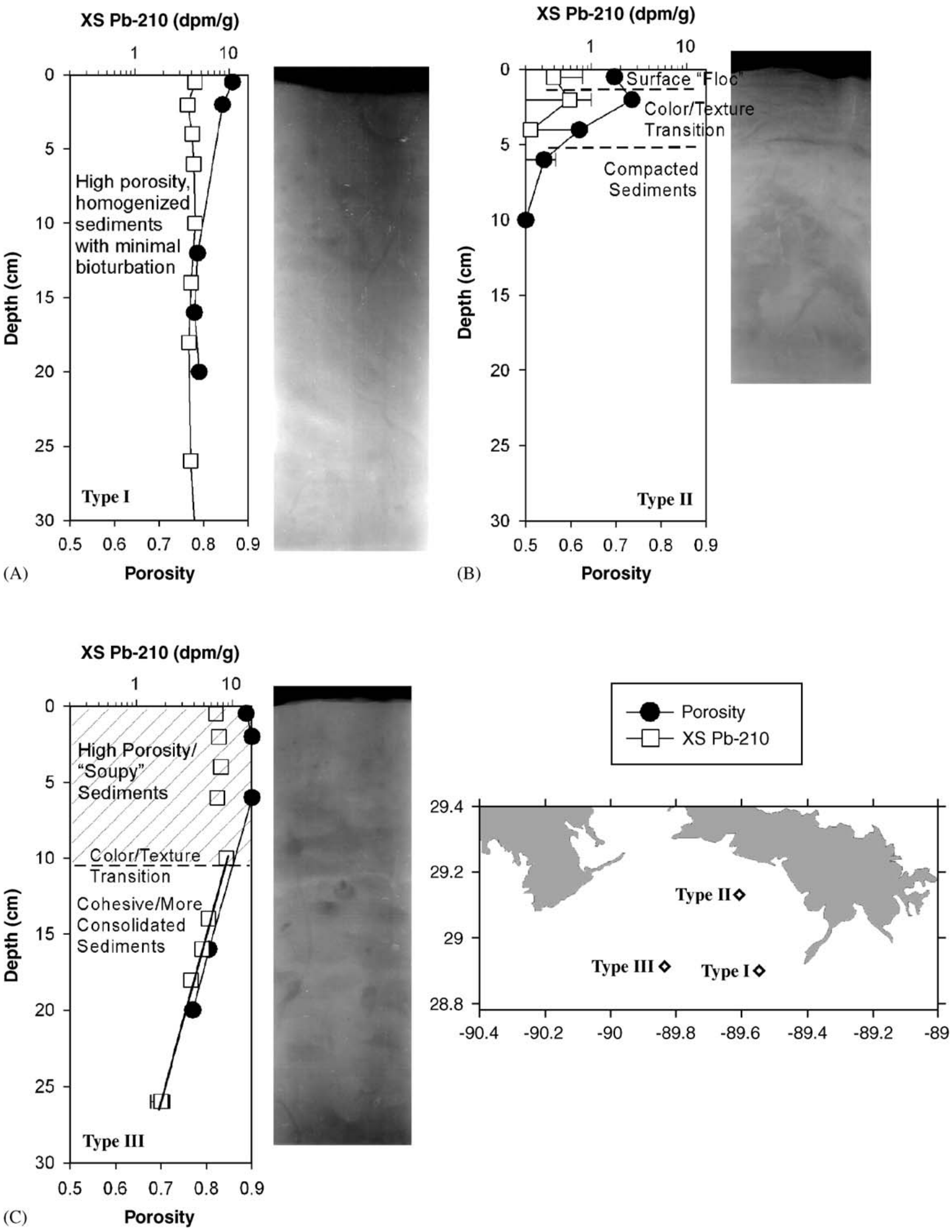


Fig. 2. Three types of $^{210}$Pb profiles used to delineate depositional environments on the shelf adjacent to Southwest Pass. Porosity profiles, core descriptions, and X-radiograph negatives provide additional data used in delineating type. Brighter layers in X-radiographs are associated with coarser sediments. (A) Type I—zone of rapid accumulation; (B) Type II—no accumulation or erosional surface; and (C) Type III—mixed surface region within an otherwise accumulating deposit. Station locations are shown in the bottom panel.

in porosity at the transition from bioturbated muds to compacted clays (typically $<10$ cm) at depth. (Fig. 2b). The most prevalent depositional environment was steady accumulating sediments beneath a thin bioturbated zone (Type III). Cores from these sites had an exponential decrease in downcore porosity and some primary structure at depth ($>10$ cm, X-radiograph) with evidence of reworking in the surface sediments (Fig. 2c).

Although most cores fit into these three designated groups easily, some cores did portray slightly different downcore trends. Several $^{210}$Pb profiles had a stair-step downcore trend, potentially associated with flooding events. These stair-stepped profiles were only evident in box cores collected near Southwest Pass during the LaSER cruise, but have since been recognized in recent kasten cores collected in the same vicinity and more subtle downcore changes in excess $^{210}$Pb further afield (Allison unpublished data; Corbett unpublished data). The observed rapid change in downcore excess $^{210}$Pb activity in these cores is most likely associated with Mississippi River flood or major storm events. Cores collected closer to the river mouth would have a more pronounced change in downcore activity due to the increased amount of sediment delivered and a potential increase in grainsize. In addition, the reduction in particle residence time within the water column will reduce the exposure to $^{210}$Pb-rich marine water, resulting in a low $^{210}$Pb deposit (Sommerfield and Nittrouer, 1999).

Since many of the same sites were re-occupied during the four different cruises included in this data set, plotting the depositional environment type for each station provides both a spatial and

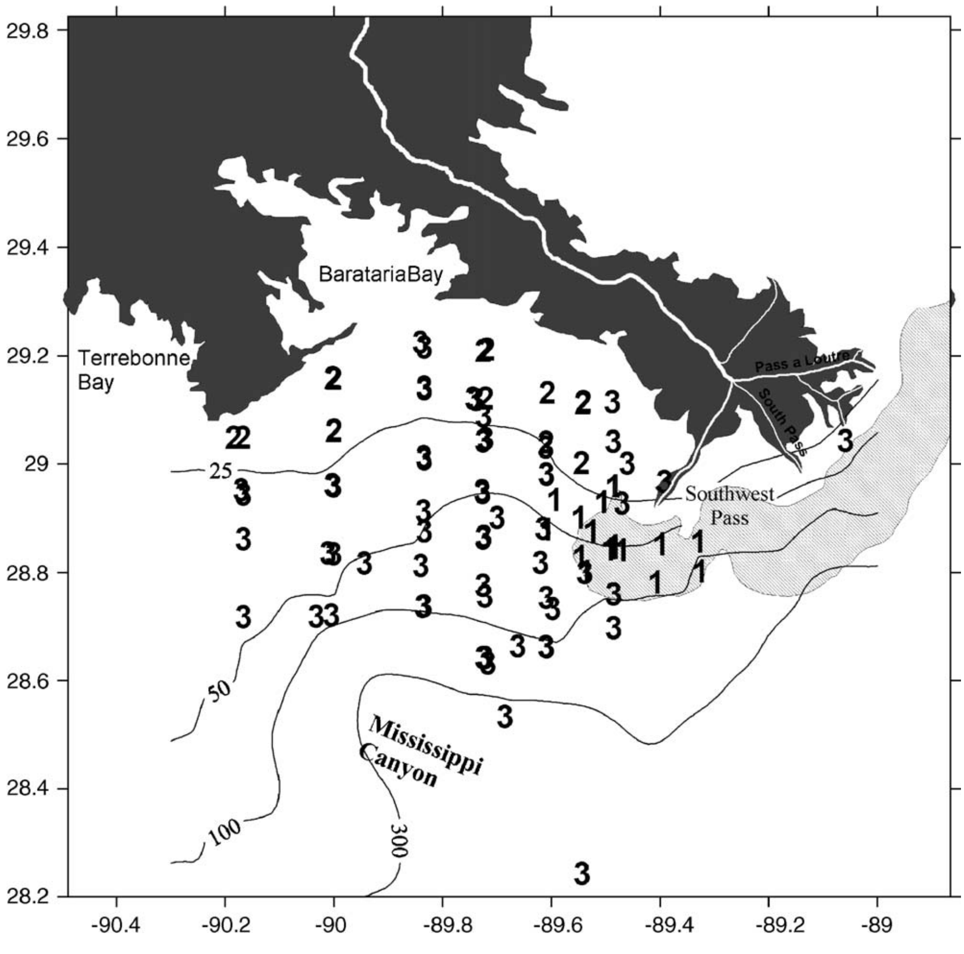


Fig. 3. Regional distribution of $^{210}$Pb profile type (interpreted depositional environment) as determined from box cores for each cruise. All cruises are plotted to demonstrate the consistency with time (1988–2000). Numbers refer to the environment type (refer to Fig. 2). Hatched area represents approximate zone of mass sediment movement.

temporal framework for the shelf west of Southwest Pass (Fig. 3). The spatial distribution of depositional types is quite distinct and does not change significantly with time. Type I sites are primarily located proximal to Southwest Pass in 30–100 m of water. Prodelta mud areas are within the zone of mass movement (Fig. 3, shaded area) that produces further seaward transport of the finer-grained material (Coleman, 1981; Adams et al., 1987). This region is also expected to experience significant sediment reworking and export during the winter months (Goni et al., 1997; Huh et al., 2001; Corbett et al., 2004).

$^{210}$Pb profiles that portrayed little to no actively accumulating sediments (Type II) were found in most nearshore ($<20$ m water depth) cores, with the exception of an area just south of Barataria Bay that revealed a steady-state profile beneath a $\sim$5-cm thick mixed layer (Type III). Coastal erosion and subsidence in this region is exposing old deltaic muds deposited as prodeltas associated with the Lafourche delta (2500–800 yrs BP; Penland et al., 1988). The sharp transition between the Types II and III depositional environments corresponds to the seaward extent of the Lafourche delta (Penland et al., 1988; Coleman, 1988) and represents a "mudline" between modern sediments beyond the 20 m contour and relic deltaic deposits. The remainder of the shelf (distal of Southwest Pass) is characterized by the Type III depositional environment.

### 4.2. Geographic distribution of sediment accumulation

The results of this study allow for the first representation of a shelf-wide decadal-scale sediment accumulation map for the region west of Southwest Pass. A decrease in accumulation rate and concomitant increase in the influence of bioturbation distally from the prodelta muds was first recognized by Moore and Scruton (1957). The decrease in accumulation rates and seaward fining grain size on the shelf opposite the delta was initially explained by hydraulic sorting from differential particle settling. However, more recent studies have recognized that fine-grained riverine sediments can be trapped near the upper delta front by particle aggregation (Trefry et al., 1994), only to be remobilized along- and across-shelf by variable bottom shear stress induced by winter frontal passages (Corbett et al., 2004) and sediment instability (Coleman et al., 1998b and references therein).

Sediment accumulation rates calculated from box cores and available kasten cores throughout the study area provide a regional and, in some cases, a temporal perspective (Fig. 4). As expected, the highest rates of accumulation were found near Southwest Pass in the area recognized by Corbett et al. (2004) as a zone of rapid deposition of river-borne particles. This area is also dominated by the Type I environment; due to the rapid deposition and the limited depth that the box cores penetrate into the sediments, most $^{210}$Pb profiles from this region could not be used to calculate an accumulation rate. Type I environments that had nearly vertical excess $^{210}$Pb profiles were not used to construct the regional accumulation map. However, several kasten cores were collected in this area and are included in the accumulation distribution. However, this area of near vertical $^{210}$Pb profiles is also associated with sediment mass movement (refer to Fig. 3, hatched area) and therefore may be more suspect for accumulation. If cores were collected in active flows, the profiles would certainly have a vertically disturbed profile. However, the mass movement also occurs in the form of slide blocks that retain their stratigraphy. Regardless, most areas in this setting (e.g., inside the area of mass movement), will have multiple sediment sources that will only complicate the $^{210}$Pb record. For this study, accumulation rates calculated in this area are considered maximum rates.

Three cross/along-shelf transects illustrate the variability of accumulation rates and depth of mixing along the shelf (Fig. 5). Sediment accumulation rates decrease fairly rapidly west of the Type I environment area. The E–W transect (Fig. 5, middle panel) portrays the more traditional "Mississippi Model" of a prodelta with declining accumulation rates moving away from Southwest Pass (Moore and Scruton, 1957; Trefry et al., 1994). The first four sites along this transect are within the zone of initial river-borne sediment deposition (as defined by Corbett et al., 2004) and exhibit the highest accumulation rates. A kasten core (250 cm) collected at EW-2 provides a much longer record of deposition and is in agreement with box cores collected in the same vicinity. The marked change in depositional environment (Fig. 3) and accumulation rate (Figs. 4 and 5) occurs beyond 30 km west of Southwest Pass. The E–W transect shows a transition from near vertical $^{210}$Pb profiles to a more

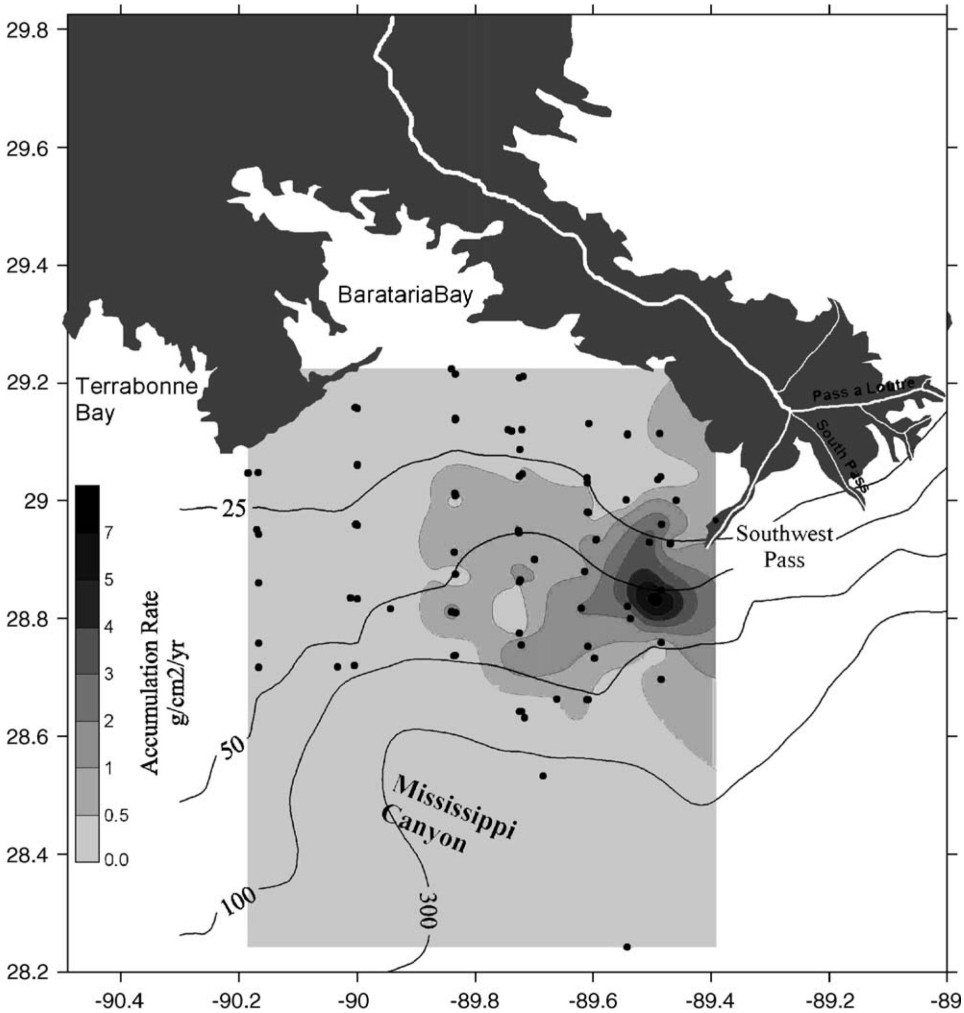


Fig. 4. Geographic distribution of accumulation rates ($g\,cm^{-2}\,yr^{-1}$) across the deltaic region. Rates are calculated from both box and kasten cores. Closed circles are coring sites included in the contour calculation. Type I environments from box cores (refer to Fig. 3) were not included in the contour.

exponential decay beneath a surface mixed layer. This same transition is evident by the dramatic decrease in sediment accumulation rate from EW-4 ($2.2\,g\,cm^{-2}\,yr^{-1}$) to EW-5 ($0.5\,g\,cm^{-2}\,yr^{-1}$). Again, this major change is a function of rapid settling of particles from the river plume and/or delivery from the river within the benthic boundary layer (Corbett et al., 2004), which limits rapid transport down the face of the delta front.

The CHIRP seismic transect collected almost along this same E–W line shows a similar transition in sediment accumulation rate (Figs. 6 and 7). In the first 10–15 km of the interpreted line, subbottom penetration is limited by shallow biogenic gas formation associated with rapid sediment loading and degradation of riverine and plume-derived (biogenic) organic matter. This zone also corresponds to the region where mass movement is active; marked by sudden variations in bottom topography created by slumps and slides (Fig. 6). Beyond this region, several eastward-dipping reflectors are evident and can be traced along most of the line west of the gas charged zone. Kasten cores collected during the ICC study in 2003 (data not shown here) at 14 km ("proximal" site) and 37 km ("mid" site) along this same line allow age estimates of four seismic horizons (A–D) using a $^{210}Pb$-derived geochronology. The thickness of sediments above and the age at the horizon are utilized to provide an estimate of sediment accumulation rate along the entire length of the line (Fig. 7). The sediment accumulation rates of corresponding

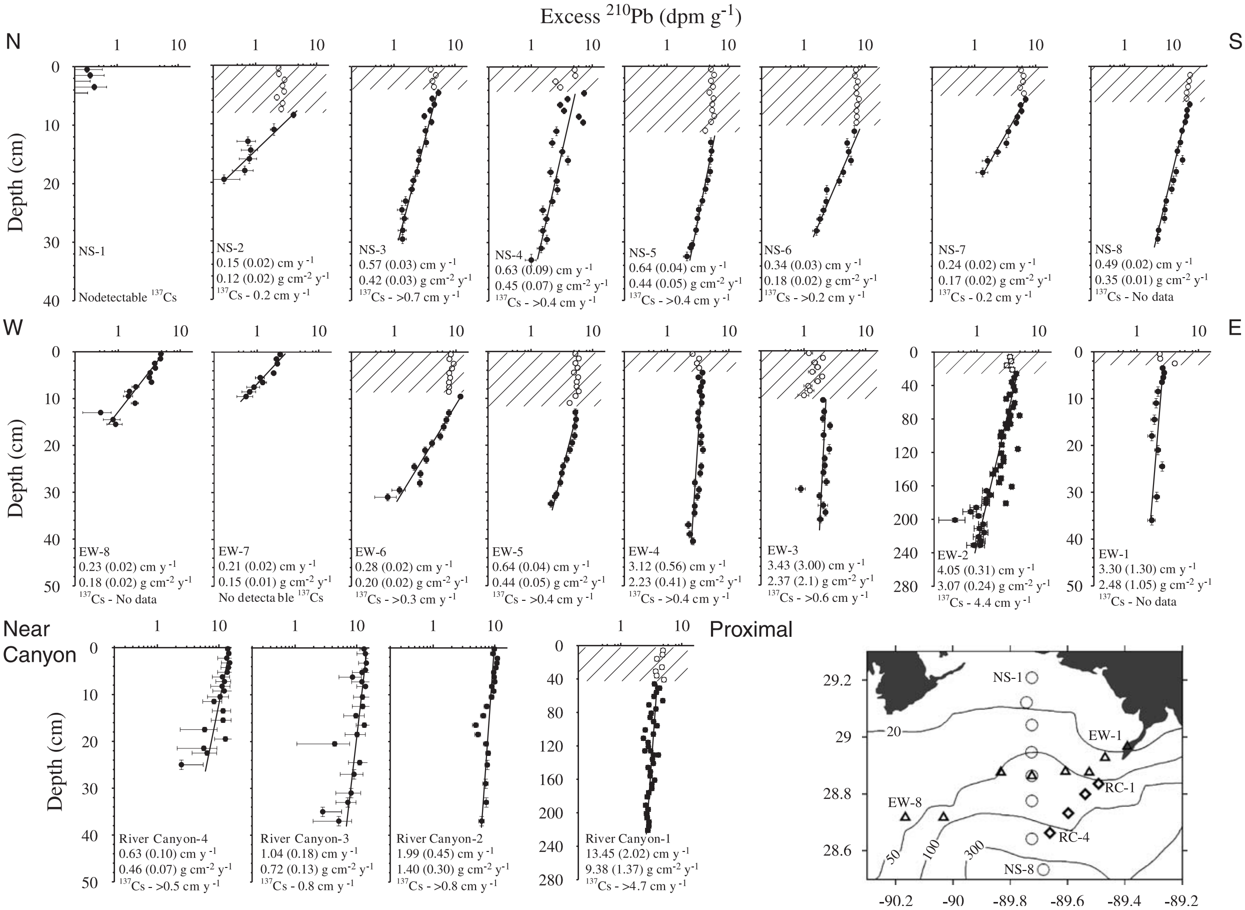


Fig. 5. Excess $^{210}Pb$ activities and calculated sediment accumulation rates from $^{210}Pb$ and $^{137}Cs$ for three cross/along shelf transects (refer to inset for station locations). Confidence limits for calculated rates are shown in parentheses. $^{137}Cs$ accumulation rates are reported as greater than (>) if activity was present at the bottom of the profile. $^{137}Cs$ accumulation rates are in good agreement with $^{210}Pb$-determined rates. The River–Canyon transect (bottom panel) refers to the southern CHIRP seismic line (Fig. 1). Hatched lines are interpreted as a mixing layer and are not included in the sediment accumulation rate calculations. All data points have errors plotted. Counting error was typically <7% and therefore many error bars are similar in size to the data point. Note that NS-5 and EW-5 is the same core.

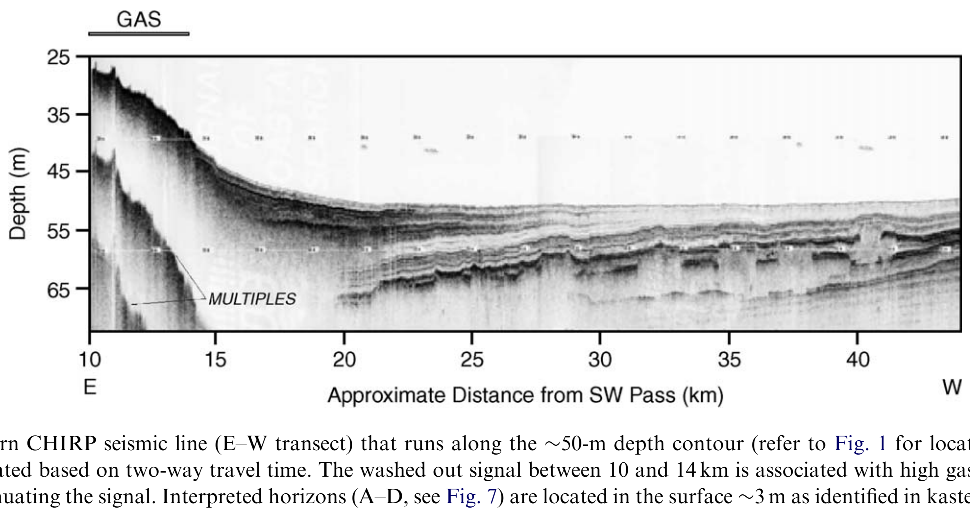


Fig. 6. Northern CHIRP seismic line (E–W transect) that runs along the ~50-m depth contour (refer to Fig. 1 for location). Sediment depth is calculated based on two-way travel time. The washed out signal between 10 and 14 km is associated with high gas content in the sediments attenuating the signal. Interpreted horizons (A–D, see Fig. 7) are located in the surface ~3 m as identified in kasten cores located at 15 and 37 km from SW Pass.

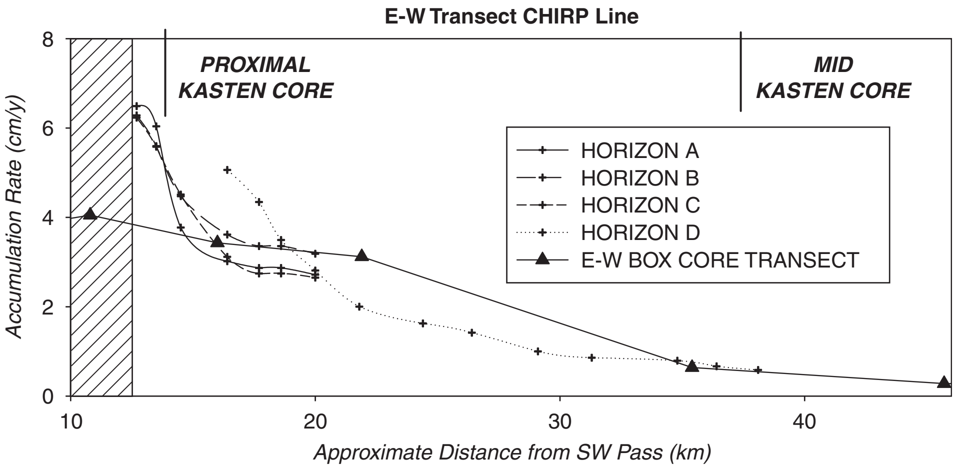


Fig. 7. Interpreted sediment accumulation rates along the E–W transect CHIRP line. CHIRP accumulation rates are calculated based on the $^{210}$Pb-calculated age of different horizons (A–D) from kasten cores collected along the same line (core locations shown at the top of graph). Accumulation rates for horizon A–C are based on age dates from the Proximal kasten core, while horizon D rates are based on the Mid Site kasten core. Calculated sediment accumulation rates from box cores collected along the E–W transect are also plotted for comparison (triangles; from Fig. 5, middle panel). Hatched area represents zone of signal attenuation in CHIRP seismic profile.

boxcore $^{210}$Pb stations along the E–W transect have also been included in this seismic interpretation (Fig. 7). This continuous along-transect seismic estimate displays the same basic pattern of rapidly declining sediment accumulation rates in approximately the same area as seen in the regional accumulation contours (Fig. 4) and the E–W transect cores (Fig. 5, middle panel) for each horizon mapped. This suggests that this sediment accumulation pattern has been present for many decades, although the interpreted accumulation rates of horizon D (deepest/oldest or the reflectors) are much greater than those estimated for horizons A–C. This may indicate a slight decrease in the rate through time and may be a result of decreased sediment delivered to the Mississippi delta in the last century due to the construction of dams, diversions, and levees.

The N–S transect is approximately 35 km from SW Pass. Most of the coring sites on this transect display a surface mixed layer on the order of 5–10 cm thick above a zone of exponential decay (Type III) with the exception of NS-1 (northernmost site). NS-1 is typical of many of the shallow water sites (Type II) with low/no excess $^{210}$Pb activities ($\leqslant 0.4\,\mathrm{dpm\,g^{-1}}$), low porosity, and nearly vertical profiles. In addition, a majority of the cores collected in this environment were $<25$ cm in length due to the compacted clays encountered near surface. Accumulation rates increase from this nearshore area to the 50–60 m depth contour. The highest rates of sediment accumulation on this transect are approximately $0.6\,\mathrm{cm\,yr^{-1}}$ ($0.4\,\mathrm{g\,cm^{-2}\,yr^{-1}}$; Fig. 5 top panel) and are most likely associated with river-derived sediments. Corbett et al. (2004) showed this area to be at the edge of the region of initial deposition of river-borne sediments. South of this area, accumulation rates decrease to $0.24\,\mathrm{cm\,yr^{-1}}$ ($0.17\,\mathrm{g\,cm^{-2}\,yr^{-1}}$) before doubling to $0.49\,\mathrm{cm\,yr^{-1}}$ ($0.35\,\mathrm{g\,cm^{-2}\,yr^{-1}}$) at the southernmost site on this transect. This increase in accumulation rate may be associated with a preferential pathway of sediment dispersal toward the Mississippi Canyon, or it may merely reflect spatial variability of accumulation on the shelf.

Like the E–W transect, the River–Canyon transect shows a decreasing rate of accumulation from Southwest Pass to the Canyon (Fig. 5, bottom panel). The highest sediment accumulation rate (Canyon-1; $13.4\,\mathrm{cm\,yr^{-1}}$; $9.4\,\mathrm{g\,cm^{-2}\,yr^{-1}}$) was found along this transect (50 m water depth) in an area noted as the primary depocenter for river-borne particles. Corbett et al. (2004) measured short-term deposition rates as high as $36\,\mathrm{cm\,yr^{-1}}$ ($25\,\mathrm{g\,cm^{-2}\,yr^{-1}}$) based on $^{7}$Be ($t_{1/2} = 53.3$ days) in this same area. The high accumulation rates are also recorded in slump basins (Fig. 8, inset; Allison unpublished data), a product of sediment instability. Although these slump basins may receive lateral fluxes associated with mass movement and river flux, cores collected from these basins may provide the best possible assessment of deposition and

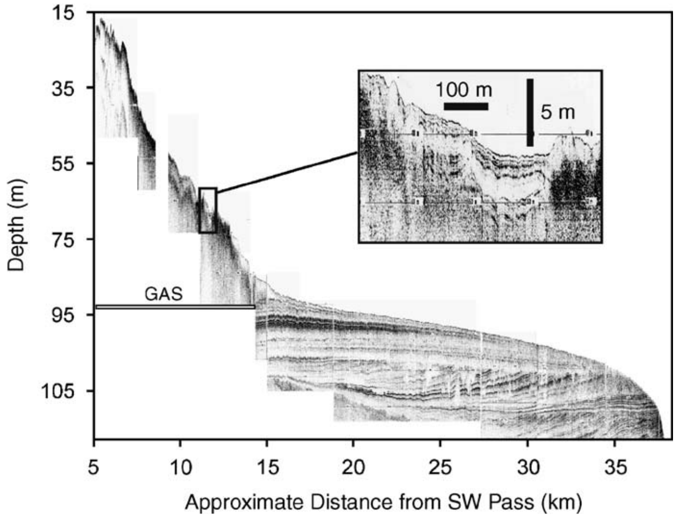


Fig. 8. Southern CHIRP seismic line from Southwest Pass to the edge of the Mississippi Canyon (River–Canyon transect; refer to Fig. 1 for location). Sediment depth is calculated based on two-way travel time. The washed out signal between 5 and ~15 km is associated with high gas content in the sediments attenuating the signal. Interpreted horizons (1–3; see Fig. 9) are located in the surface ~3 m as identified in kasten cores located at 16 and 24 km from SW Pass. Inset shows recent deposition within a small slump basin. Note the stair-step features along the surface of the gas region.

accumulation rates in this area, since mass movement processes are less likely to generate post-depositional disturbance (note horizontal reflectors in the CHIRP profile). A kasten core collected in this slump basin had an accumulation rate of 6.5 cm yr$^{-1}$ (4.7 g cm$^{-2}$ yr$^{-1}$). It is these high rates of deposition in conjunction with the efficient degradation of organic matter (Aller, 1998) that leads to bed instability and downslope mass movement. Further evidence of the extent of sediment instability and mass movement can be seen in the River–Canyon CHIRP line (Fig. 8). There are two characteristics in the first 10 km of the line that suggest this zone is strongly overprinted by sediment instability and mass movement. First, the attenuated signal is a function of rapid biochemical degradation of organic material leading to the formation of large quantities of gas. The gas formation contributes to the excess pore pressures that lead to sediment destabilization (Coleman et al., 1998b). Secondly, the bathymetry generated by the seismic line has a stair-step appearance along the first 10 km (slope of shelf in this area is ~0.4°), potentially attributed to subaqueous slides and slump blocks. A similar bottom morphology was documented south of South Pass with fathometer profiles (Coleman et al., 1998b). Many of the scarps documented in their study were traceable for several kilometers, and we assume that this is also the case in our study region.

Beyond the gas-charged zone, several subbottom reflectors are evident along the CHIRP line and can be used to provide an estimate of accumulation rate (Figs. 8 and 9). All the rates calculated for the different horizons agree closely with one another and with box cores collected along the same line. Unlike the E–W transect CHIRP line, there does not seem to be a decrease in sediment accumulation rate with time. On the contrary, the box cores and the Horizon 1 provide some of the highest rates along this line. This provides additional support of differential modern sediment delivery to different regions of the shelf. Along-isobath sediment movement occurs by normal resuspension processes west of the delta, whereas delivery of sediments along the canyon transect may be additionally influenced by mass movement events on varying timescales.

### 4.3. Sediment budget

The Mississippi deltaic system has been described as a low energy environment with bed shear stresses typically less than that necessary to remobilize sediments (Adams et al., 1987; Wiseman and Dinnel, 1988; Wright and Nittrouer, 1995). However, increased energy during the fall and winter months is sufficient to remobilize and transport sediment west of the area of rapid deposition (Corbett et al., 2004; Dail et al., 2004). In addition, Coleman et al. (1998b) suggested that as much as

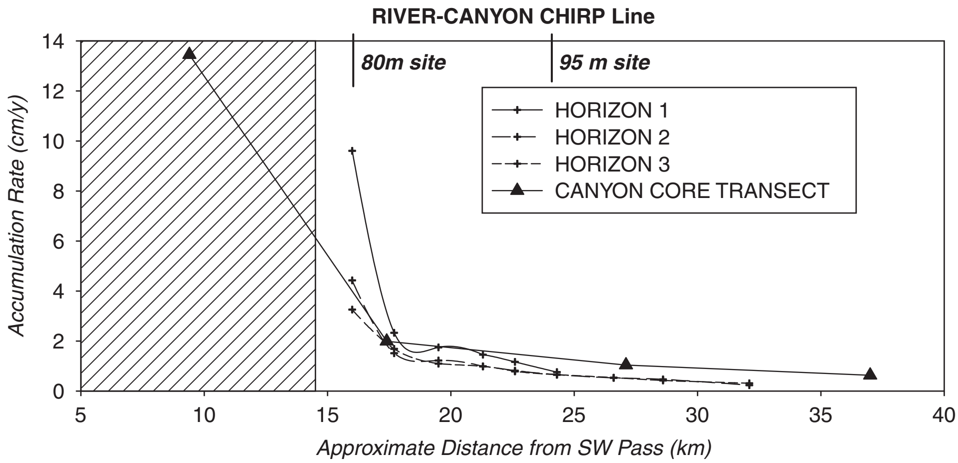


Fig. 9. Interpreted accumulation rates along the River–Canyon transect CHIRP line. Sesimic accumulation rates are calculated based on the $^{210}$Pb-calculated age of different horizons (1–3) from kasten cores collected at two stations (80 and 95 m sites) along the same line (core locations shown at the top of graph). Accumulation rates for horizon 1 are based on age dates from the 80 m site kasten core, while horizon 2–3 rates are based on the 95 m site kasten core calculated sediment accumulation rates from box cores collected along this transect are also plotted for comparison (triangles; from Fig. 5, bottom panel). Hatched area represents zone of signal attenuation in CHIRP seismic profile.

Table 1
Summary of data used to estimate the sediment budget for the shelf adjacent to the Mississippi River delta

| Accumulation rate region (cm yr$^{-1}$)[a] | Average accumulation rate (g cm$^{-2}$ yr$^{-1}$) | Area (km$^2$) | Mass accumulation (T/yr$^{-1}$) | Percent of total |
|---|---|---|---|---|
| >7.0 | 9.5 | 10 | $1.0 \times 10^6$ | 2 |
| 5.0–7.0 | 6.9 | 30 | $2.1 \times 10^6$ | 5 |
| 4.0–5.0 | 4.7 | 50 | $2.3 \times 10^6$ | 6 |
| 3.0–4.0 | 3.8 | 110 | $4.1 \times 10^6$ | 10 |
| 2.0–3.0 | 2.4 | 240 | $5.9 \times 10^6$ | 15 |
| 1.0–2.0 | 1.5 | 560 | $8.2 \times 10^6$ | 20 |
| 0.5–1.0 | 0.72 | 1550 | $11.2 \times 10^6$ | 28 |
| <0.5 | 0.16 | 3440 | $5.5 \times 10^6$ | 14 |
| | | | $40.3 \times 10^6$ | 100 |

The average accumulation rates are based on box and kasten cores.
[a]Refer to Fig. 4.

40% of the sediment that is annually deposited on the delta-front is transported downslope by short-term mass movement processes. Although the modern and historic sediment accumulation processes have been thoroughly documented for the Mississippi delta, a modern sediment budget is lacking for this region. The radiochemical and seismic data presented provides a valuable resource to generate a first order sediment budget for the continental shelf adjacent to the Mississippi River delta.

The amount of sediment accumulating within our study area west of the birdfoot delta was determined by contouring the mass accumulation rate at each site and multiplying the area between contours by the average accumulation rate for that interval (Table 1). Accumulation rates near the delta used in this budget are based on kasten cores and box cores that portrayed a steady-state profile beneath a mixed layer (Type III). Box cores that had a zone of rapid accumulation (Type I) were not used in these calculations. The area contoured was bounded by the ~10 m contour to the north, Southwest Pass to the east, ~100 m contour to the south, and a longitude of 90.2 W to the west, due to the limited data beyond these boundaries. The calculated annual amount of sediment deposited on the continental shelf west of the Mississippi River delta is $4.0 \pm 0.9 \times 10^{13}\,\mathrm{g\,yr^{-1}}$ ($40 \times 10^{6}\,\mathrm{t\,yr^{-1}}$). Following Jaeger et al. (1998), the confidence limit was estimated based on the standard error of the regression line used to calculate the mass accumulation rate (<18%) and the fit of the contoured data relative to the measured rates (<7%). Accumulation rates for the area near the delta are considered maximum values. However, the amount of material deposited in this area is minimal compared to the remainder of the study region. Majority of the sediment (>75%) is accumulating beyond the region of rapid deposition of river-borne particles and mass movement, so the error associated with this estimate is assumed to be small relative to the total budget.

The amount of sediment delivered annually to the Northern Gulf of Mexico by the Mississippi River is approximately $1.3\text{–}1.5 \times 10^{14}\,\mathrm{g}$ ($130\text{–}150 \times 10^{6}\,\mathrm{t}$; Milliman and Meade, 1983; Meade and Parker, 1985; Meade, 1996; Mossa, 1996). This sediment load estimate is based on a long term average (>17-years) and is post 1963, as dramatic reductions in sediment load are observed when comparing the period before 1963 and the early 1970s (Mossa, 1996). Although sediments are sometimes stored in the lower 500 km of the river seasonally, there is no evidence for longer-term storage (Galler and Allison, submitted for publication). Therefore, the sediment load measured at Tarbert Landing is a fair estimate for the amount of material delivered annually to the continental shelf through the bird-foot delta. Our study region receives majority of its sediment load from Southwest Pass. River water, and the corresponding sediment load, moves through three main distributary channels, e.g. Southwest Pass, South Pass, and Pass a Loutre. Approximately 50% of the discharged material from the Mississippi is delivered west of the delta, entering our study region, while the remaining 50% flows to the south and east (US Army Corps of Engineers, 1974), although it may enter our study region depending on local currents at the time of discharge. Based on these assumptions, the Mississippi River delivers between 65 and 75 million metric tons of material into our study region; therefore, the amount of material accumulating accounts for approximately 50–60% of that delivered. This suggests that a significant amount of the sediment exiting the delta toward the west is advected beyond the study region on a decadal timescale. Corbett et al. (2004) used short-lived radionuclides ($^{234}$Th, $^{7}$Be, $^{137}$Cs) to demonstrate that most river-borne material is initially deposited within 30 km of the delta, but increased wind/wave forcing during the winter months potentially remobilizes and transports the material away from the deltaic region. Our data further substantiate this observation, indicating that just under half of the sediment delivered to this region is only stored near the delta temporarily, presumably followed by transport alongshore or off-shelf.

## 5. Summary

This study examined $^{210}$Pb data from 92 cores collected during the last decade covering much of the shelf (<150 m water depth) adjacent to the west side of the Mississippi delta. This data provides a unique and invaluable insight into the spatial and modern temporal variations of sediment accumulation in this dynamic deltaic system. As summarized below, the $^{210}$Pb profiles provide new information about the varying depositional environments and mechanisms of sediment supply.

(A) Three depositional environments were recognized throughout the shelf based on the shapes of $^{210}$Pb activity profiles. In most cases these could be divided into (1) a zone of rapid accumulation; (2) an erosional surface reworked by waves and currents with no accumulation; or (3) a mixed surface region overlying an accumulating deposit. These different styles of deposition offer insight into the sediment processes and depositional environments that occur along the shelf.

(B) Accumulation rates near Southwest Pass in the zone of river-derived sediment deposition and potential sediment mass movement and instability are typically $>2.5\,\mathrm{cm\,yr^{-1}}$ ($>1.8\,\mathrm{g\,cm^{-2}\,yr^{-1}}$). Two kasten cores (~200 cm in length) collected near Southwest Pass also indicate rapid deposition ($>4\,\mathrm{cm\,yr^{-1}}$; $3\,\mathrm{g\,cm^{-2}\,yr^{-1}}$) on a longer timescale than that captured in the box cores. Accumulation rates for many box cores collected in this zone could not be calculated due to near vertical $^{210}$Pb profiles. Nearshore (<20 m), profiles are dominated by mixing of a thin surface layer, probably reworked by waves and currents, and little to no accumulation with the exception of an area just south of Barataria Bay that have steady-state profiles. Accumulation rates for many of these sites could not be calculated due to the lack of excess $^{210}$Pb. Accumulation rates for the distal shelf are typically $<0.7\,cm\,yr^{-1}$ ($<0.5\,g\,cm^{-2}\,yr^{-1}$) and dominated by apparent steady-state accumulation beneath a $\sim$10 cm mixed layer.

(C) $^{210}$Pb accumulation rates and interpreted CHIRP transects suggests two separate mechanisms of sediment delivery to the shelf. Sediments in the area west of Southwest Pass are supplied primarily from resuspension/remobilization processes that move sediments in the primary direction of the dominant alongshore current (along-isobath). In contrast, sediments are supplied to the region south and southwest of Southwest Pass by subaqueous slides and slumps, thereby providing higher rates of accumulation farther from the sediment source (cross-isobath).

(D) A preliminary sediment budget based on calculated regional accumulation rates indicates that 40–50% of the sediment delivered annually by the river west of the birdsfoot delta is subsequently transported out of the study area, presumably along and across shelf.

## Acknowledgments

We gratefully acknowledge the captain and crew of the R/V *Pelican* for their assistance in field sampling. We would also like to thank Pete Swarzenski, Greg Booth, Dan Duncan, Rodney Powell, Ryan Clark, and Mike Stewart for their help in core collection, sampling, and analyses. We thank Andrea Ogston, Steve Kuehl, and an anonymous reviewer for their comments, which greatly improved this manuscript. Support of this research was provided by the National Science Foundation, Department of Defense through the Tulane/Xavier Center of Bioenvironmental Research, National Oceanographic and Atmospheric Administration, and the Louisiana Board of Regents.

## References

Adams, C.E., Roberts, H.H., 1993. A model of the effects of sedimentation rate on the stability of Mississippi Delta sediments. Geo-Marine Letters 13, 17–23.

Adams, C.E., Wells, J.T., Coleman, J.M., 1982. Sediment transport on the central Louisiana continental shelf: Implications for the developing Atchafalaya River Delta. Contributions in Marine Science 25, 133–148.

Adams, C.E., Swift, J.P., Coleman, J.M., 1987. Bottom currents and fluviomarine sedimentation on the Mississippi prodelta shelf: February–May 1984. Journal of Geophysical Research 92, 14595–14609.

Aller, R.C., 1998. Mobiel deltaic and continental shelf muds and suboxic, fluidized bed reactors. Marine Chemistry 61, 143–155.

Aller, R.C., 2001. Transport and reactions in the bioirrigated zone. In: Boudreau, B.P., Jorgensen, B.B. (Eds.), The Benthic Boundary Layer. Oxford University Press, New York, pp. 269–301.

Allison, M.A., Kineke, G.C., Gordon, E.S., Goni, M.A., 2000. Development and reworking of a seasonal flood deposit on the inner continental shelf off the Atchafalaya River. Continental Shelf Research 20, 2267–2294.

Appleby, P.G., Oldfield, F., 1992. Application of Pb-210 to sedimentation studies. In: Ivanovich, M., Harmon, R.S. (Eds.), Uranium-Series Disequilibrium: Applications to Earth, Marine, and Environmental Problems, second ed. Clarendon Press, Oxford, UK, pp. 731–778.

Benninger, L.K., Aller, R.C., Cochran, J.K., Turekian, K.K., 1979. Effects of biological mixing on the $^{210}$Pb chronology and trace metal distribution in a Long Island Sound sediment core. Earth and Planetary Science Letters 43, 241–259.

Berner, R.A., 1982. Burial of organic carbon and pyrite sulfur in the modern ocean: its geochemical and environmental significance. American Science 282, 451–473.

Berner, R.A., 1989. Biogeochemical cycles of carbon and sulfur and their effect on atmospheric oxygen over Phanerozoic time. Paleogeography, Paleoclimatology and Paleoecology 73, 97–122.

Cable, J., Burnett, W., Moreland, S., Westmoreland, J., 2001. Empirical assessment of gamma ray self-absorption in environmental analyses. Radioactivity and Radiochemistry 12, 30–39.

Cho, K., O Reid, R., Nowlin Jr., W.D., 1998. Objectively mapped stream function fields on the Texa-Louisiana shelf based on 32 months of moored current meter data. Journal of Geophysical Research 103 (C5), 10377–10390.

Cochrane, J.D., Kelly, F.J., 1986. Low-frequency circulation on the Texas-Louisiana continental shelf. Journal of Geophysical Research 91 (C9), 10645–10659.

Coleman, J.M., 1981. Deltas: Processes of Deposition and Models for Exploration, second ed. International Human Resources Development Corporation, Boston, Mass.

Coleman, J.M., 1988. Dynamic changes and processes in the Mississippi River delta. Geological Society of America Bulletin 100, 999–1015.

Coleman, J.M., Gagliano, S.M., 1964. Cyclic sedimentation in the Mississippi River deltaic plain. Transactions of the Gulf Coast Association of Geological Society 14, 67–80.

Coleman, J.M., Roberts, H.H., Stone, G.W., 1998a. Mississippi River Delta: an overview. Journal of Coastal Research 14 (3), 698–716.

Coleman, J.M., Walker, H.J., Grabau, W.M., 1998b. Sediment instability in the Mississippi River Delta. Journal of Coastal Research 14 (3), 872–881.

Corbett, D.R., McKee, B., Duncan, D., 2004. An evaluation of mobile mud dynamics in the Mississippi River deltaic region. Marine Geology 209, 91–112.

Cutshall, N.H., Larsen, I.L., Olsen, C.R., 1983. Direct analysis of $^{210}$Pb in sediment samples: self-adsorption corrections. Nuclear Instruments and Methods 206, 309–312.

Dagg, M., Benner, R., Lohrenz, S., Lawrence, D., 2004. Transport and transformation of dissolved and particulate materials on continental margins influenced by major rivers: benthic boundary layer and seabed processes. Continental Shelf Research 24, 833–858.

Dail, M.B., Corbett, D.R., McKee, B.A., Duncan, D., 2004. High frequency time-series of the dynamic sedimentation processes on the western shelf of the Mississippi River Delta. Eos Transactions on AGU, 85(47), Fall Meeting Supplement Abstract OS41D-0512.

Fisk, H.N., McFarlan Jr., E., Kolb, C.R., Wilbert Jr., L.J., 1954. Sedimentary framework of the modern Mississippi delta. Journal of Sedimentary Petrology 24, 76–99.

Flynn, W.W., 1968. The determination of low levels of polonium-210 in environmental materials. Analytica Chimica Acta 43, 221–227.

Galler, J.J., Allison, M.A., submitted. Seasonal variability of shallow-water mud storage on the lower Mississippi River channel bed. Geology.

Goldberg, E.D., Koide, M., 1962. Geochronologocal studies of deep-sea sediments by the ionium-thorium method. Geochimica Cosmochimica Acta 26, 417–450.

Goni, M.A., Ruttenberg, K.C., Eglinton, T.I., 1997. Sources and contribution of terrigenous organic carbon to surface sediments in the Gulf of Mexico. Nature 389, 275–278.

Huh, O.K., Walker, N.D., Moeller, C., 2001. Sedimentation along the eastern Cheneir Plain coast: down drift impact of a delta complex shift. Journal of Coastal Research 17, 72–81.

Jaeger, J.M., Nittrouer, C.A., Scott, N.D., Milliman, J.D., 1998. Sediment accumulation along the glacially impacted mountainous coastline: north–east Gulf of Alaska. Basin Research 10, 155–173.

Keown, M.P., Dardeau Jr., E.A., Causey, E.M., 1986. Historic trends in the sediment flow regime of the Mississippi River. Water Resources Research 22, 1555–1564.

McKee, B.A., Nittrouer, C.A., DeMaster, D.J., 1983. Concepts of sediment deposition and accumulation applied to the continental shelf near the mouth of the Yangtze River. Geology 11, 631–633.

McKee, B.A., Aller, R.C., Allison, M.A., Bianchi, T.S., Kineke, G.C., 2004. Transport and transformation of dissolved and particulate materials on continental margins influenced by major rivers: benthic boundary layer and seabed processes. Continental Shelf Research 24, 899–926.

Meade, R., 1995. Contaminants in the Mississippi River. US Geological Survey Circular 1133. Reston, Virginia.

Meade, R.H., 1996. River-sediment inputs to major deltas. In: Milliman, J., Haq, B. (Eds.), Sea-Level Rise and Coastal Subsidence. Kluwer, London, pp. 63–85.

Meade, R., Parker, R., 1985. Sediment in rivers of the United States. In: National Water Summary 1984. US Geological Survey, Water Supply Paper 2275. pp. 49–60.

Milliman, J.D., Meade, R.H., 1983. World-wide delivery of river sediment to the oceans. Geology 91, 1–21.

Moore, D.G., Scruton, P.C., 1957. Minor internal structures of some recent unconsolidated sediments. Bulletin of the American Association of Petrological Geology 41, 2723–2751.

Mossa, J., 1996. Sediment dynamics in the lowermost Mississippi River. Engineering Geology 45, 457–479.

Neill, C.F., Allison, M.A., 2005. Subaqueous deltaic formation on the Atchafalya Shelf, Louisiana. Marine Geology 214, 411–430.

Nittrouer, C.A., Sternberg, R.W., Carpenter, R., Bennett, J.T., 1979. The use of $^{210}$Pb geochronology as a sedimentological tool: an application to the Washington continental shelf. Marine Geology 31, 297–316.

Nittrouer, C.A., DeMaster, D.J., McKee, B.A., Custhall, N.H., Larsen, L.I., 1984. The effect of sediment mixing on $^{210}$Pb accumulation rates for the Washington continental shelf. Marine Geology 31, 297–316.

Penland, S., Boyd, R., 1981. Shoreline changes on the Louisiana barrier coast. IEEE Oceans 81, 209–219.

Penland, S., Boyd, R., Suter, J.R., 1988. Transgressive depositional systems of the Mississippi delta plain: a model for barrier shoreline and shelf sand development. Journal of Sedimentary Petrology 58, 932–949.

Presley, B.J., Trefry, J., Shokes, R., 1980. Heavy metal inputs to Mississippi delta sediments. Water, Air, and Soil Pollution 13, 481–494.

Prior, D.B., Coleman, J.M., 1978. Disintegrating retrogressive landslides on a very-low-angle subaqueous, Mississippi delta. Marine Geotechnology 3, 37–60.

Roberts, H., Suhayda, J.N., Coleman, J.M., 1980. Sediment deformation and transport on low-angle slopes: Mississippi River delta. In: Coates, D.R., Vitek, J.D. (Eds.), Threshholds in Geomorphology. Allen and Unwim, London, pp. 131–167.

Sommerfield, C.K., Nittrouer, C.A., 1999. Modern accumulation rates and a sediment budget for the Eel shelf: a flood-dominated depositional environment. Marine Geology 154 (1-4), 227–241.

Trefry, J.H., Metz, S., Nelson, T.A., Trocine, R.P., Eadie, B.J., 1994. Transport of particulate organic carbon by the Mississippi River and its fate in the Gulf of Mexico. Estuaries 17, 839–849.

Trowbridge, A.C., 1930. Building the Mississippi delta. American Association of Petroleum Geologists Bulletin 14, 867–901.

US Army Corps of Engineers, 1974. Deep draft access to the ports of New Orleans and Baton Rouge. Draft Environmental Statement, New Orleans District.

Wiseman, W.J., Dinnel, S.P., 1988. Shelf currents near the mouth of the Mississippi River. Journal of Physical Oceanography 18, 1287–1291.

Wright, L.D., Coleman, J.M., 1974. Mississippi River mouth processes: effluent dynamics and morphologic development. Journal of Geology 82, 751–778.

Wright, L.D., Nittrouer, C.A., 1995. Dispersal of river sediments in coastal seas—6 contrasting cases. Estuaries 18, 494–508.